



Modeling of photodegradation process to remove the higher concentration of environmental pollution

Yadollah Abdollahi^{a,b,*}, Azmi Zakaria^{b,*}, Suhana Binti Mohd Said^a, Mohd Faizul Bin Mohd Sabri^c, Nor Asrina Sairi^d, Majid Rezayi^d, Ebrahim Abouzari-lotf^e, Masoumeh Dorraj^d, Aminul Islam^f

^aFaculty of Engineering, Department of Electrical Engineering, University of Malaya, 50603 Kuala Lumpur, Malaysia, Tel. +60 389 467 503; Fax: +60 389 467 102; email: yadollahabdollahi@yahoo.com (Y. Abdollahi)

^bMaterial Synthesis and Characterization Laboratory, Institute of Advanced Technology, Universiti Putra Malaysia, 43400 Serdang, Selangor, Malaysia, Tel. +60 389 466 650; Fax: +60 389 454 454; email: azmizak@upm.edu.my (A. Zakaria)

^cFaculty of Engineering, Department of Mechanical Engineering, University of Malaya, 50603 Kuala Lumpur, Malaysia

^dFaculty of Science, Department of Chemistry, University of Malaya, 50603 Kuala Lumpur, Malaysia

^eInstitute of Hydrogen Economy, Energy Research Alliance, International Campus, Universiti Teknologi Malaysia, 54100 Kuala Lumpur, Malaysia

^fFaculty of Science, Catalysis and Science Research Center, University Putra Malaysia, UPM, 43400 Serdang, Selangor, Malaysia

Received 5 October 2014; Accepted 15 March 2015

ABSTRACT

Environmental organic pollutants are mineralized to harmless final-products such H₂O and CO₂ by photocatalytic advanced oxidation processes (AOPs). In photocatalytic-AOPs, an appropriate concentration of *p*-Cresol was mixed with certain amount of ZnO in 500 mL deionized water according to an experimental-design. Then the mixture was irradiated by UV-A lamp at different pH for 6 h. At specific time intervals, the sampling was carried out to calculate the efficiency of the photodegradation. Therefore, the photodegradation as a system consists of four input variables such irradiation time, pH, amount of ZnO and *p*-Cresol's concentration while the only output was the efficiency. In this work, the system was modeled and optimized by semi-empirical response surface methodology. To obtain the empirical responses, the design was performed in laboratory. Then observed responses were fitted with several well-known models by regression process to suggest a provisional model. The suggested model which was validated by several statistical evidence, predicted the desirable condition with higher efficiency. The predicted condition consisted of irradiation time (280 min), pH (7.9), photocatalyst (1.5 g L⁻¹), *p*-Cresol (95 mg L⁻¹) and efficiency (95%) which confirmed by further experiments. The closed confirmation results has presented the removal (efficiency = 94.7%) of higher *p*-Cresol concentration (95 mg L⁻¹) at shorter irradiation time in comparison with the normal photodegradation efficiency (97%) which included irradiation time (300 min), pH (7.5), photocatalyst amount (1.5 g L⁻¹) and

*Corresponding authors.

Presented at the International Conference on Business, Economics, Energy and Environmental Sciences (ICBEEES) 19–21 September 2014, Kuala Lumpur, Malaysia

p-Cresol (75 mg L^{-1}). As a conclusion, the modeling which is able to industrial scale up succeeded to remove higher concentration of environmental organic pollutants with ignorable reduction of efficiency.

Keywords: Multivariate-modeling; Optimization; Photodegradation; AOPs; Photocatalyst; ZnO; Organic-pollutant; Water treatment; RSM; Environment

1. Introduction

Well over 90% of untreated wastewater that contains organic pollutants such as phenolic compounds is flowing into rivers, lakes and highly productive coastal zones; hence, the effective methods to remove the pollutants have been attracted attention [1]. The methods are including biological oxidation systems, electrochemical techniques, physical adsorption methods and advanced oxidation processes (AOPs) [2–7]. However, the biological methods are slow, selective, pH and temperature sensitive [8,9]. The chemical methods are unable to mineralize all the organics and also generate new environmental pollutants [10]. The physical methods such as adsorption techniques are not able to remove the hazardous from the environment. Among them, the AOPs mineralize the organics to environmental friendly final-products such H_2O and CO_2 using a non-toxic semiconductors as suspended photocatalyst [11–14]. The promising approach is to use the photocatalyst for producing the carrier pairs (e^- and h^+) such as excited electrons and remained holes that are generated by a light irradiation source. The carriers are driven to the surface of the photocatalyst and then into the interface layers in suspended solution [15–18]. The layers are placed between solid (catalyst) and liquid phases (aqueous pollutants) which contain H_2O and dissolved oxygen molecules. The oxygen traps the excited electrons and converts it to " O_2^- " product that is very reactive species. On the other hand, remained holes are reduced by H_2O and may be organic pollutants in higher concentration [19]. The species are converted to hydroxyl radical ($\cdot\text{OH}$) which is powerful and non-selective agent to oxidize the organic pollutants and their probable intermediates [16,20,21]. The layers are affected by four initial factors such as pH, amount of the suspended photocatalyst and pollutants concentration as input variables which change the efficiency of the photodegradation as final output. The pH of the liquid phase affects the layers' electrical charges; the amount of the catalyst and the pollutants changes the number of active site in the layers [22–24]. Moreover, irradiation time is another effective variable that generates the carrier pairs. Obviously, to enhance the efficiency, it needs to optimize the input variables.

However, the optimization is quite complicated because it contains the calculation of mass transfer, mechanism of the reactions, kinetic evaluation, and the balance of radiant energies that have been irritating tragedies for the traditional methods such as one variable at a time [20,21,25–27]. Recently, multivariate methods such as response surface methodology (RSM) has been accepted for modeling of the productive processes to optimize the input variables and achieve the optimal yield of production as output without the mentioned complexities [28]. The modeling is a semi-empirical technique that uses experimental results, and a group of mathematical and statistical algorithms [29]. As it is reported, modeling has successfully maximized the efficiency of several photodegradation such as methylparaben, phenol and azo dye [30–32]. As objectives of this work, the photodegradation was modeled by RSM. For the modeling, the experiments were designed to obtain the matrix of the variables such as irradiation time, pH, the photocatalyst amount and concentration of pollutant while the only response was the efficiency of the photodegradation. To calculate the efficiencies as responses, the design was performed in laboratory according to the following methodology. The observed responses were used for regression and fitting process to find the suitable provisional model for the photodegradation. The model was validated by using several statistical techniques in analysis of variance (ANOVA). The validated model obtained the optimized values of the variables which maximized the efficiency of the photodegradation. As final achievement, the model predicted the desirable condition including minimum standard error and the maximum efficiency which were validated by further experiments.

2. Experimental

2.1. Materials and methods

The used chemicals were including ZnO (99%, Merck). *p*-Cresol (99.5%, Fluka), NaOH (99% Merck), H_2SO_4 (95–97%) and other required materials were obtained from Merck, and were used without further purification. To obtain the actual responses, the design of the experiment (Table 1) was performed in

Table 1

The CCD experimental-design of the photodegradation, x_1 , x_2 , x_3 and x_4 are the input variables, Y_a and Y_p are actual and model predicted output respectively, the residuals are the difference between Y_a and Y_p

Run	x_1	x_2	x_3	x_4	Y_a (%)	Y_p (%)	Residual
1	180	6	1	50	46.21	46.00	0.21
2	300	6	1	50	64.9	63.29	1.61
3	180	9	1	50	69.81	70.63	-0.82
4	300	9	1	50	84.88	86.67	-1.79
5	180	6	2	50	64.73	66.13	-1.40
6	300	6	2	50	90.04	92.67	-2.63
7	180	9	2	50	75.27	75.50	-0.23
8	300	9	2	50	99.98	100.79	-0.81
9	180	6	1	100	35.19	35.29	-0.10
10	300	6	1	100	55.88	55.83	0.05
11	180	9	1	100	58.54	58.67	-0.13
12	300	9	1	100	78.08	77.96	0.12
13	180	6	2	100	34.89	33.67	1.12
14	300	6	2	100	63.4	63.46	-0.06
15	180	9	2	100	42.21	41.79	0.42
16	300	9	2	100	72.88	70.33	2.55
17	120	7.5	1.5	75	47.23	45.38	1.85
18	360	7.5	1.5	75	91.48	91.21	0.27
19	240	4.5	1.5	75	25.31	23.54	1.77
20	240	10.5	1.5	75	55.4	55.04	0.36
21	240	7.5	0.5	75	70.04	70.04	0.00
22	240	7.5	2.5	75	84.11	82.54	1.57
23	240	7.5	1.5	25	94.91	96.38	-1.47
24	240	7.5	1.5	125	52.95	55.21	-2.26
25	240	7.5	1.5	75	98.62	96.83	1.79
26	240	7.5	1.5	75	97.13	96.83	0.30
27	240	7.5	1.5	75	98.07	96.83	1.24
28	240	7.5	1.5	75	96.53	96.83	-0.30
29	240	7.5	1.5	75	97.08	96.83	0.25
30	240	7.5	1.5	75	97.93	96.83	1.10

laboratory by using a non-continuous binary photoreactor which identified in our previous work [16]. According to the design, known amount of *p*-Cresol and ZnO were mixed to make a litter suspension that was irradiated by an UV-A lamp (6 W). The intensity of the light source peaked at 365 nm. To maintain suspension throughout the photoreactor, the solutions were magnetically stirred. In order to liberate any CO₂ formed, oxygen availability and fluidization of solution, air was blown into the solution by an air-pump with flow rate 150 Lh⁻¹. The temperature of the solution was maintained at 25°C by following cool water into the binary of the photoreactor [25]. To evaluate the degradation, the samples were withdrawn from the bulk solution during performance and filtered through a 0.45 μm polytetrafluoro-ethylene

membrane [16]. To measure the unreacted *p*-Cresol, the absorbance of solutions was recorded by Shimadzu, UV-1650PC UV-Visible spectrometer, at 277 nm that is maximum wavelength of the Cresol [25]. The observed results in the laboratory were used to calculate the efficiency as actual response that applied for fitting process and modeling. The calculation method was reported by our previous work [25].

2.2. The experimental design

As Table 1 shows, the experiments were designed by central composite design (CCD) that is default of Design-Expert software version 8.0.7.1, Stat-Ease Inc., USA [33]. As initial information, the level of the effective variables were selected in vicinity of the photodegradation efficiency according to previous work [25]. In the design, the number of experiments was 30 which consist of the factorial points (16), the axial points (8) and the replications (6). The replications are used to measure experimental error. Table 2 shows the variables and also their used levels in the design. In Table 1, each row presents an experiment that contains the run number, variable (x_i) and observed output (actual responses).

3. A brief theory of RSM

RSM creates a functional relationship between variable–variable and variables–response by using approximated low-degree polynomial models that consist of the variables and their coefficients. Eq. (1) shows the second-order polynomial which RSM commonly uses for optimization process [34],

$$Y = \beta_0 + \sum_{i=1}^n \beta_i x_i + \sum_{i=1}^n \beta_{ii} x_i^2 + \sum_{i=1}^{n-1} \sum_{j=i+1}^n \beta_{ij} x_i x_j + \varepsilon \quad (1)$$

where Y is the interested response, β_0 is a constant term, β_i is the coefficient of the linear terms, β_{ii} represents the coefficient of the quadratic terms, β_{ij} is the coefficient of the interaction terms while x_i are control variables and “ ε ” is a random experimental error [35]. To estimate the β 's, RSM fitting process provides the sufficient data by regression technique [36,37]. In the process, the actual responses from performance of the experimental design are fitted to the linear, two-factor interaction (2FI), quadratic and cubic models by sequential model sum of squares (SMSS) [36,37]. The results of the SMSS are compared to select the provisional model for the system. In this case the system is photodegradation. The SMSS compares the sufficiency

Table 2

The effective variables in code and actual value and their used level for CCD experimental design of the photodegradation

Effective variables		Level of variables				
		($-a$)	Low	Center	High	($+a$)
Code						
values		-2	-1	0	1	2
X_1	Irradiation-time, min	120	180	240	300	360
X_2	pH	4.5	6	7.7	9	10.5
X_3	Photocatalyst, g L^{-1}	0.5	1	1.5	2	2.5
X_4	p -Cresol, mg L^{-1}	25	50	75	100	125

of the models using the statistical significance of adding new model terms, step-by-step in increasing order [38]. The comparison is presented by statistical evidence such as the F -value, predicted residual sum of squares (PRESS), adjusted R -squared (R_{Adj}), predicted R -squared (R_{Pred}), and probability value (p -value). The PRESS is the sum of the squares of a model's prediction errors. The minimum value of the p -value and PRESS as well as the maximum value of R_{Adj} , R_{Pred} , and F -value are considered to determine the provisional model of the process [39]. The provisional model is usually suggested by the software and is studied in detail by using ANOVA [40]. The ANOVA indicates the significance of each term of the model, including the intercept, linear, interaction, and square terms. In fact, the adequacy of the model such as importance of the terms is certified by ANOVA and then the model is used to navigate the process (in this case photodegradation). The model is able to track the optimum amount of the variables in the experimental design points by canonical and 3D plots as points and surface response respectively. Moreover, the model predicts the desirable condition that selected by experimenter to maximize the yield of the process (in this case, the efficiency of the photodegradation).

4. Results and discussion

4.1. Photodegradation modeling

In the modeling process, the obtained actual responses of performed experimental design (Table 1) were fitted with linear, 2FI, quadratic and cubic models to calculate residuals. The residual values shows the difference between actual responses and the models predicted responses which were based of SMSS evaluation and model selection [36,37]. Table 3 shows the statistical evidences of the models that originated based on the residuals. As observed, standard

deviation (std. dev.) of the quadratic model that indicates the outlier of the actual responses was minimum in comparison with other models [41]. Moreover, its lack of fit's F -value and p -value were very small and too large respectively which show the actual responses are fit with quadratic model. In addition, the R_{Adj} (1.00) was in reasonable agreement (<0.20) with R_{Pred} (0.999) as well as maximum R^2 and minimum PRESS also belong to the model. As a summary of the fitting process, the SMSS comparison for 2FI, linear, quadratic and cubic models is presented by Table 4 that illustrates the merit of the quadratic model. Therefore, the statistical evidence has confirmed the sufficiency of the quadratic model and it was suggested as provisional model to validate in details by using ANOVA.

4.2. The model validation

The provisional model presents the relationship between irradiation time, pH, amount of the photocatalyst and concentration of p -Cresol as effective variables and the efficiency as interested response (Eq. (2)),

$$\begin{aligned}
 Y = & -602.66146 + 1.004x_1 + 108.590x_2 + 113.696x_3 \\
 & + 1.478x_4 - 1.736E - 3x_1x_2 + 0.072x_1x_3 \\
 & + 6.458E - 4x_1x_4 - 4.375x_2x_3 - 2.500E - 3x_2x_4 \\
 & - 0.393x_3x_4 - 1.996E - 3x_1^2 - 6.416x_2^2 - 20.746x_3^2 \\
 & - 9.498E - 3x_4^2
 \end{aligned} \quad (2)$$

where x_1 , x_2 , x_3 and x_4 are the input variables that have identified in Table 2 and Y is photodegradation efficiency as interested response and output. The model presents the linear parameters (x_1 , x_2 , x_3 and x_4), quadratic factors (x_1^2 , x_2^2 , x_3^2 , x_4^2) and interaction of the variables (x_1x_2 , x_1x_3 , x_1x_4 , x_2x_3 , x_2x_4 and x_3x_4) [27].

Table 3

The fit statistics and lack of fit evidence of linear, 2FI, quadratic and cubic models which obtained from fitting process

Source	Lack of fit		Model summary statistics				
	F-value	p-value	Std. dev.	R_{Adj}	R_{Pred}	R^2	PRESS
Linear	459.8	7540.85	17.4	0.487	0.405	0.336	9759.7
2FI	600.5	6893.51	19.1	0.531	0.284	0.213	11576.7
Quadratic	0.2	0.27	0.8	1.000	0.999	0.997	44.9
Cubic	1.8	14.52	1.1	0.999	0.998	0.994	89.5

Table 4

The SMSS comparison for 2FI, linear, quadratic and cubic models to suggest the provisional

Source	F-value	p-value	Remark
2FI vs. Linear	0.3	0.9307	
Quadratic vs. 2FI	1385.3	<0.0001	Suggested
Cubic vs. Quadratic	2.9	0.0925	Aliased

Generally, each parameter multiplies to individual coefficient that determined specific weight of the parameter in the model. The multiplied parameters and their multiplied weights were linked by using positive (+) and negative (-) sign. The signs affect on the slop of the response's curve synergistically or antagonistically while the weights are the importance of the parameters in the model [27]. The linear and square parameters had synergic and antagonistic effect on the response respectively while the effect of the interactions parameters was consisted of them. For example, the effect of irradiation time (x_1) on the photodegradation was analyzed in Fig. 1. As observed, the linear has presented the synergistic effect while curvature parts consisted of synergistic and antagonistic effect on the efficiency. In the model (Eq. (2)), the weights of linear and quadratic parameter for x_1 were 1.004 and 1.996E-3, respectively whereas the parameter affected synergistically (+) and antagonistically (-) on the photodegradation %. As shown the slope of linear is sharper than curvature because their weights in the model. The linear effect was demonstrated from 120 to 240 min of irradiation time which improved the photodegradation. However, the quadratic effect cooperated vice versa from 250 to 300 min.

The ANOVA indicates the significant of the each term in the model and consequently confirm the final form of the model. As Table 5 shows, the ANOVA evidence of existing terms in the provisional model.

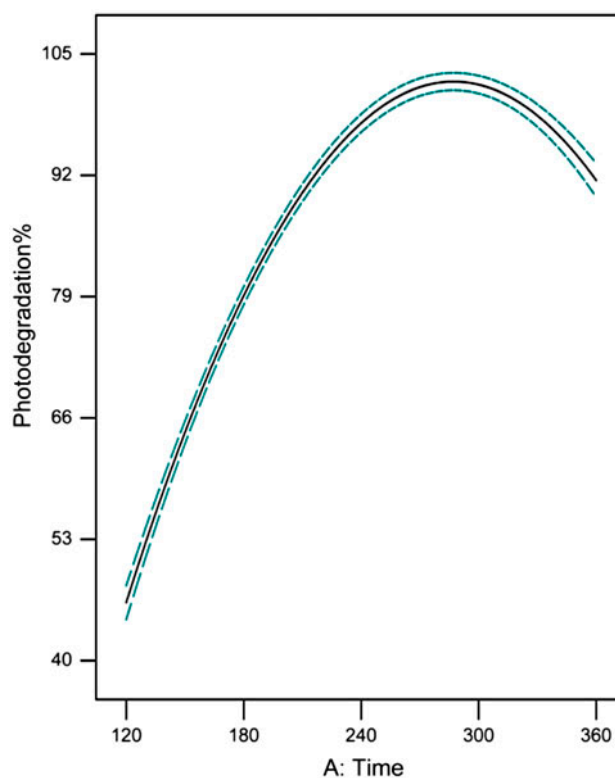


Fig. 1. The linear and quadratic effect of irradiation time (x_1) as input variable on the photodegradation efficiency as output response with error bar. The figure consists of linear and curvature parts that confirmed the effect of the irradiation time of the efficiency.

Generally, the ANOVA has confirmed great significance of the suggested model due to present high F -value, 845.09, and low p -value <0.0001. The form of the suggested model can be changed according to the ANOVA information about the terms. As shown, only x_1x_2 and x_1^2 are not-significant which could remove from the original provisional model. Therefore the new form of the final model are presented in Eq. (3),

Table 5
The ANOVA of the existing terms in suggested quadratic model, all the terms are significant except x_1x_2 and x_1^2

Source	F-value	Prob. > F	Remark
x_1	2474.12	<0.0001	Significant
x_2	1167.45	<0.0001	Significant
x_3	201.60	<0.0001	Significant
x_4	1925.27	<0.0001	Significant
x_1^2	0.31	0.5831	Not-significant
x_2^2	59.93	<0.0001	Significant
x_3^2	12.10	0.0034	Significant
x_4^2	138.77	<0.0001	Significant
x_1x_2	0.11	0.7411	Not-significant
x_1x_3	310.25	<0.0001	Significant
x_1x_4	1141.10	<0.0001	Significant
x_2x_3	4604.86	<0.0001	Significant
x_2x_4	594.34	<0.0001	Significant
x_3x_4	778.66	<0.0001	Significant

$$\begin{aligned}
 Y = & -602.66146 + 1.004x_1 + 108.590x_2 + 113.696x_3 \\
 & + 1.478x_4 + 0.072x_1x_3 + 6.458E - 4x_1x_4 - 4.375x_2x_3 \\
 & - 2.500E - 3x_2x_4 - 0.393x_3x_4 - 6.416x_2^2 - 20.746x_3^2 \\
 & - 9.498E - 3x_4^2
 \end{aligned}
 \tag{3}$$

where the terms have already been introduced by Eq. (2).

For more evaluation, the normality of residuals, constant error and residual outlier is checked by diagnostic plots such as the plots in Fig. 2. The remarkable agreement between the actual values and

the predicted values of the study was presented in Fig. 2(a) while the distance of each observation from the fitted line was plot (Fig. 2(b)). Therefore, ANOVA and diagnostic plots certified the adequacy of the quadratic model that were used to navigate the design space.

4.3. The model navigation

The model was able to optimize the variables by using canonical response and graphical plots. The canonical responses are local optimums that determine by differentiating the quadratic model (Eq. (2)) as presented by Eqs. (4)–(7),

$$[\partial Y / \partial X_1]_{X_2, X_3, X_4} = 0 \tag{4}$$

$$[\partial Y / \partial X_2]_{X_1, X_3, X_4} = 0 \tag{5}$$

$$[\partial Y / \partial X_3]_{X_1, X_2, X_4} = 0 \tag{6}$$

$$[\partial Y / \partial X_4]_{X_1, X_2, X_3} = 0 \tag{7}$$

where the terms were introduced by Table 2. In fact, canonical optimization which is a kind of one-variable-at-a-time, presents the optimum points of the input that could maximize the output. However, the graphical optimization illustrated a surface area of the optimum condition with lower standard error by using 3D plots. The plots simultaneously considered the effect of two effective variables on the output while other two parameters were kept constant that were determined by canonical optimization. As shown

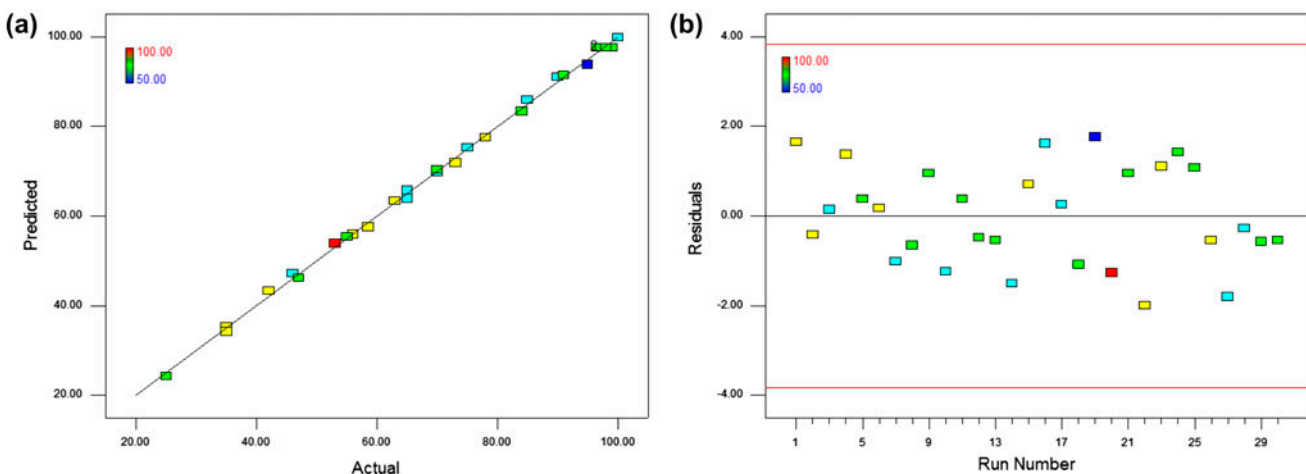


Fig. 2. The diagnostic plots of model’s significance and adequacy: (a) scatter plot of predicted values vs. actual values of the observation and (b) residual of the observation that was illustrated by residuals vs. run number.

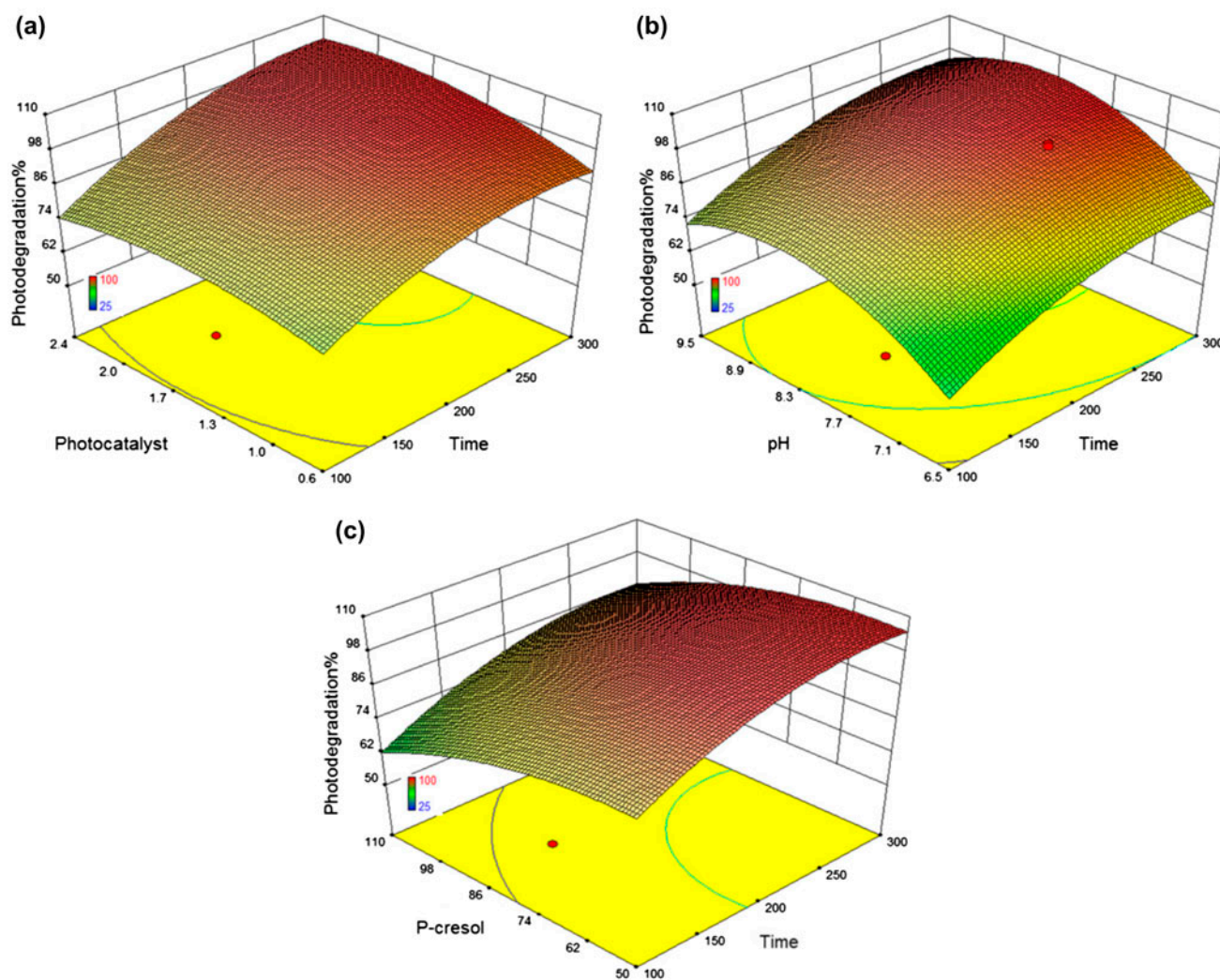


Fig. 3. The 3D plots of pH, photocatalyst and *p*-Cresol vs. the irradiation time: (a) the amount of photocatalyst was varied while pH and *p*-Cresol were kept constant at 7.5 and 75 mg L⁻¹, (b) the pH was varied while the concentration of *p*-Cresol and photocatalyst were kept constant at 75 mg L⁻¹ and 1.5 g L⁻¹ and (c) the concentration of *p*-Cresol was varied while photocatalyst and pH were kept constant at 1.5 g L⁻¹ and 7.5 respectively.

in Fig. 3, the quadratic model was able to track the behavior of the input variables during the photodegradation process. Fig. 3(a) shows the amount of photocatalyst was varied while pH and *p*-Cresol were kept constant at 7.5 and 75 mg L⁻¹ while Fig. 3(b) illustrates the pH was varied while the concentration of *p*-Cresol and photocatalyst were kept constant at 75 mg L⁻¹ and 1.5 g L⁻¹, respectively and Fig. 3(c) indicates the concentration of *p*-Cresol was varied while photocatalyst and pH were kept constant at 1.5 and 7.5 g L⁻¹. As observed, irradiation time always enhances the photodegradation when it was considered with other three variables [27]. Therefore, the variables including pH, photocatalyst and *p*-Cresol,

were studied at the end of 300 min of the irradiation time (Figs. 4–6).

Fig. 4 presents the 3D and contour plot of *p*-Cresol concentration and pH in area of the standard error which simultaneously varied at constant amount of photocatalyst (1.5 g L⁻¹). The efficiency was decreasing when the concentration of *p*-Cresol was increased in the selected pH up to 97%. This observation may be due to the fact that *p*-Cresol molecules competes with OH⁻ to attract generated h⁺ [33]. On the other hand, the efficiency was slightly enhanced with increasing pH from 6 to 7.5 also up to 97% that could be attributed to an enhancement in the number of adsorbed *p*-Cresol on the ZnO surface, ZnO and *p*-Cresol have

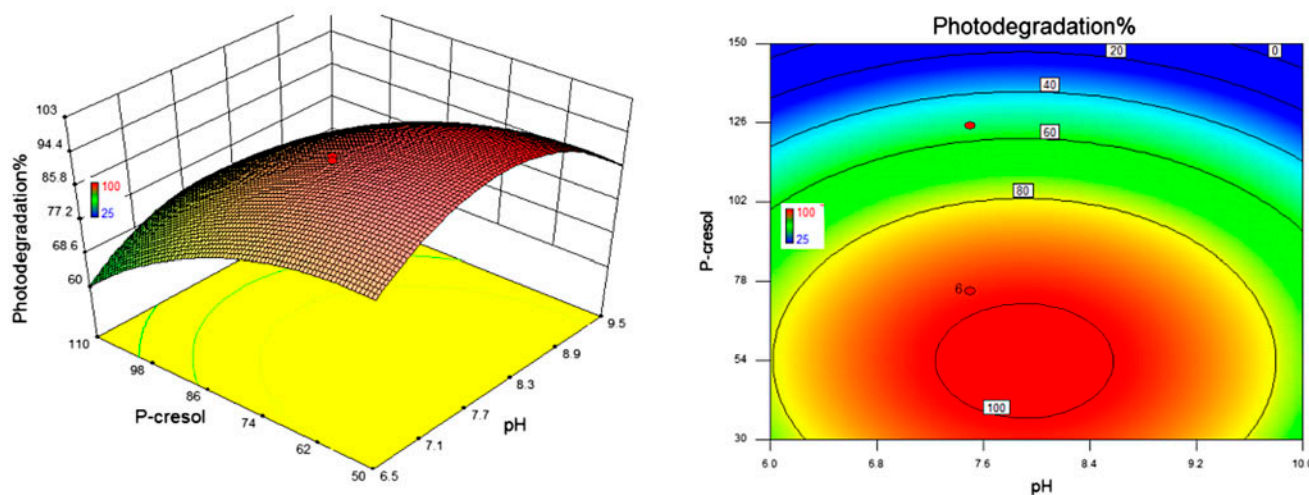


Fig. 4. The view of the 3D and contour plots of *p*-Cresol's concentration and pH at 300 min of irradiation time as variables while the amount of the catalyst was kept constant at 1.5 g L^{-1} , the level of the effective pH was illustrated 7–8.5 and maximum concentration of *p*-Cresol was 75 mg L^{-1} .

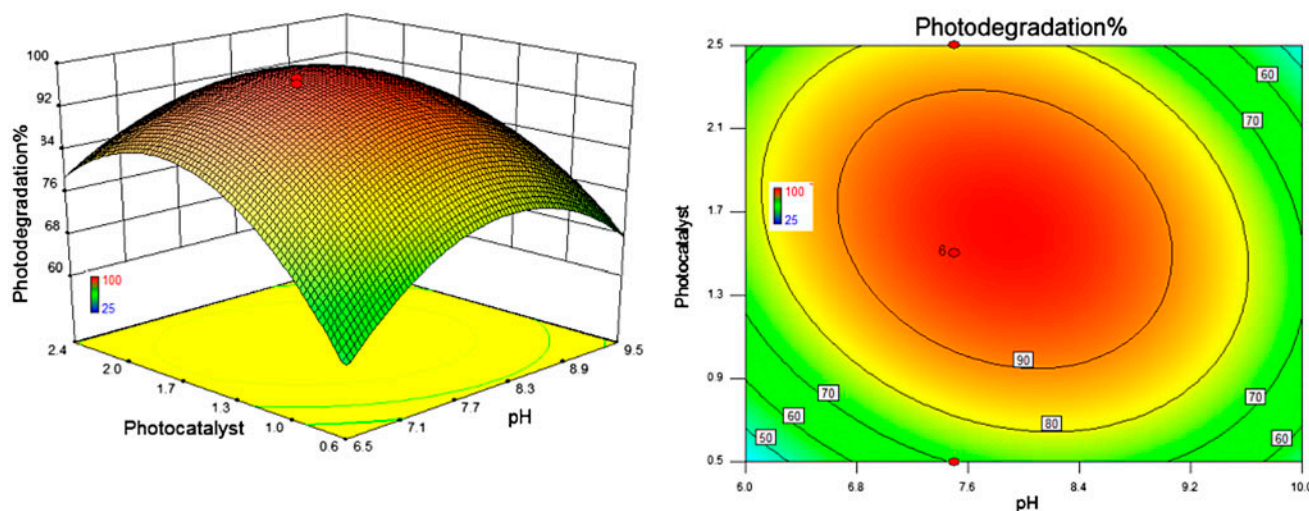


Fig. 5. The view of the 3D and contour plot of the photocatalyst amount and pH at 300 min of irradiation time while the concentration of the *p*-Cresol was kept constant at 75 mg L^{-1} , the level of the photocatalyst was determined between 0.9 and 2.3 g L^{-1} and the level of pH was 6.8–8.8 that is a little bit wider than the level that presented in Fig. 4.

different charge in this range of pH [17]. However, the efficiency was decreased above this optimum.

Fig. 5 depicts the synergy response surface photocatalyst amount (1.0 – 2.0 g L^{-1}) and pH (6 – 9) with constant *p*-Cresol concentration (75 mg L^{-1}) at the end the irradiation time. As shown, the efficiency was increased by increasing 1.0 – 1.5 g L^{-1} photocatalyst amount and pH (6 – 9). One of the reasons of the enhancement is improvement of the production of hydroxide radicals due to increase the active site of the photocatalyst. However, when the amount of

photocatalyst was increased in excess of the optimum (1.5 g L^{-1}) the efficiency decreased ($<97\%$). The reduction could be attributed to the screen effect phenomena [16].

Fig. 6 illustrates the view of the simultaneous behavior of photocatalyst (1.0 – 2.0 g L^{-1}) and *p*-Cresol (50 – 100 mg L^{-1}) at constant pH (7.5). This point of view also confirmed the optimum condition at 97% . As illustrated the photodegradation increased with increasing the photocatalyst for whole range of *p*-Cresol while it decreased with increasing *p*-Cresol

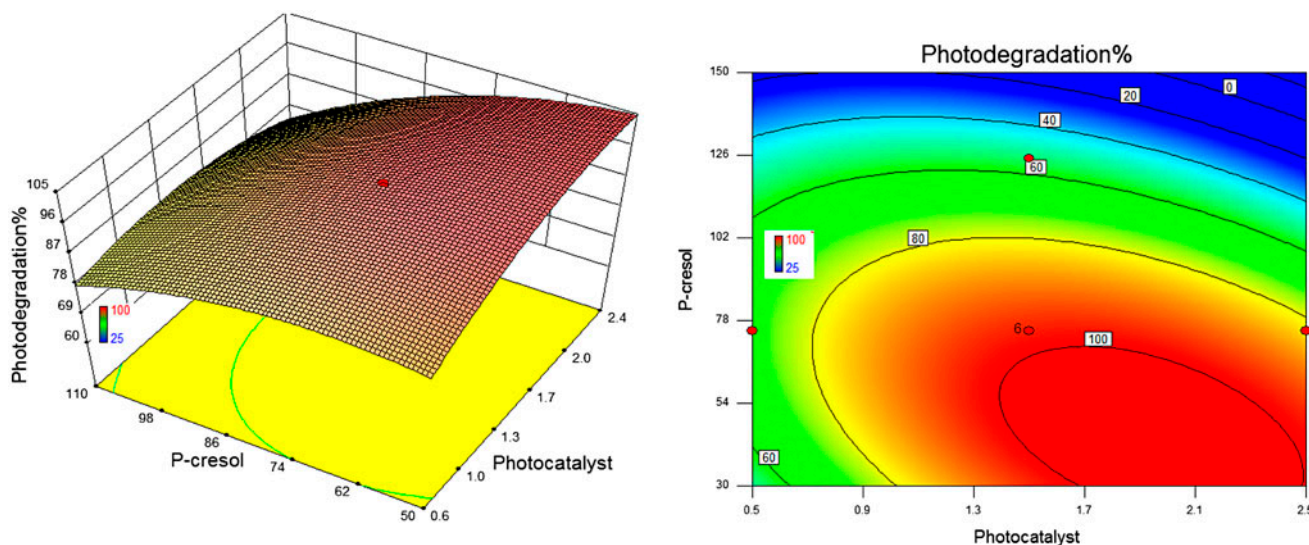


Fig. 6. The 3D and contour plots of the *p*-Cresol's concentration and photocatalyst amount at 300 min of irradiation time while the pH was kept constant at 7.5. The mentioned levels of *p*-Cresol and photocatalyst in the previous figures were confirmed.

Table 6

The comparison between the designed and model predicted the photodegradation

Process	Input variables					Output efficiency (%)
	Irradiation time (min)	<i>p</i> -Cresol (mg L ⁻¹)	Photocatalyst (g L ⁻¹)	pH		
Design	300	75	1.5	7.5		97
Prediction	280	95	1.5	7.9		94.7

for the catalysis range. As a result, the graphical optimization proved these values of input effective variables including irradiation time (240 min), pH (7.5), photocatalyst (1.5 g L⁻¹) and *p*-Cresol (75 mg L⁻¹) maximized the efficiency at 97%.

4.4. The numerical optimization

The model predicted the desirable efficiency at particular value of input variables and standard deviation by using the numerical option of the used software. The selected particular condition included irradiation time (in rang), pH (in rang), photocatalyst (in rang) *p*-Cresol (maximum), efficiency (maximum) and standard error at minimum value in the numerical software option. The model predicted condition was included the irradiation time (280 min), pH (7.9), photocatalyst amount (1.5 g L⁻¹), *p*-Cresol concentration (95 mg L⁻¹) and efficiency 95%. The desirability of the prediction was 0.921 which is quite close to 100% (at the goal). Desirability is an objective function that

uses mathematical methods to find the optimum condition. The range of the function is from zero (outside of the limit area) to one (at the goal) [33]. The condition was validated by further experiments which confirmed the prediction. The practical results of the efficiency (94.7%) were very close to the predicted value. As Table 6 shows, *p*-Cresol concentration (95 mg L⁻¹) in the model prediction was higher than the concentration in the designed while the time of the irradiation was decreased and the amount of the photocatalyst was kept constant. At this desirable condition the efficiency was not reduced which it may be due to select the proper pH (7.9) that increases generation of hydroxyl radicals (.OH) [24].

5. Conclusion

The process of *p*-Cresol photodegradation was carried out in ZnO suspension and under UV irradiation according to an experimental design. The design consisted of four variables such irradiation time, pH, the

amount of ZnO and *p*-Cresol's concentration and the efficiency as response. The design was performed to calculate the efficiencies that were used for modeling process by RSM to suggest a suitable model of the photodegradation. As a result, quadratic model was suggested as provisional model then it was validated by ANOVA. The validated model was a mathematic equation that used to optimize the variables included irradiation time, pH, amount of ZnO and *p*-Cresol's concentration based on maximized efficiency. In the level of the experimental design, the optimum values of the variables were included irradiation time (300 min), pH (7.5), photocatalyst (1.5 g L^{-1}) and *p*-Cresol (75 mg L^{-1}) which created the efficiency 97%. Moreover, the model predicted the desirable efficiency by a particular condition which included, irradiation time (in rang), pH (in rang), photocatalyst (in rang) *p*-Cresol (maximum) and efficiency (maximum) as output while standard error was at minimum value. The predicted condition included irradiation time (280 min), pH (7.9), photocatalyst (1.5 g L^{-1}) *p*-Cresol (95 mg L^{-1}), efficiency (95%) and standard error was at minimum value (0.2). The prediction was confirmed by further experiments and presented the efficiency (94.7%) That was very close to the predicted value (95%). As observed, *p*-Cresol concentration (95 mg L^{-1}) in the model prediction was higher than the concentration in the designed experiment while the time of the irradiation was less than the design. The amount of the photocatalyst was kept constant. Therefore, RSM succeeded to model the photodegradation process to enhance the efficiency of the higher concentration of environmental pollutants.

Acknowledgments

The authors wish to acknowledge the University of Malaya-Ministry of Higher Education Grant UM.C/625/1/HIR/MOHE/ENG/29, University of Malaya Research Grant (UMRG) RP014C-13AET, Fundamental Research Grant Scheme (FRGS) with project no.: FP011-2014A and Science Fund with project no.: SF020-2013.

References

- [1] The United Nations World Water Development Report, 2012. Available from: <http://www.unwater.org/statistics_pollu.html#sthash.T7Q1BYzl.dpuf>.
- [2] P. Ahamad, A. Kunhi, Degradation of phenol through ortho cleavage pathway by *Pseudomonas stutzeri* strain SPC2, *Lett. Appl. Microbiol.* 22 (1996) 26–29.
- [3] P. Ahamad, A. Kunhi, Degradation of high concentrations of cresols by *Pseudomonas* sp. CP4, *World J. Microbiol. Biotechnol.* 15 (1999) 321–323.
- [4] J.A. Müller, A.S. Galushko, A. Kappler, B. Schink, Anaerobic degradation of *m*-Cresol by desulfobacterium cetonicum is initiated by formation of 3-hydroxybenzylsuccinate, *Arch. Microbiol.* 172 (1999) 287–294.
- [5] D. Rajkumar, K. Palanivelu, Electrochemical degradation of cresols for wastewater treatment, *Ind. Eng. Chem. Res.* 42 (2003) 1833–1839.
- [6] D. Marković, B. Jokić, Z. Šaponjić, B. Potkonjak, P. Jovančić, M. Radetić, Photocatalytic degradation of a dye using TiO₂ nanoparticles immobilized on recycled wool-based nonwoven material, *CLEAN–Soil Air Water* 41 (2013) 1002–1009.
- [7] K. Parveen, U. Rafique, S.Z. Safi, M.A. Ashraf, A novel method for synthesis of functionalized hybrids and their application for wastewater treatment, *Desalin. Water Treat.* (2015) 1–10, doi: 10.1080/19443994.2015.1006819.
- [8] O. Aviam, G. Bar-Nes, Y. Zeiri, A. Sivan, Accelerated biodegradation of cement by sulfur-oxidizing bacteria as a bioassay for evaluating immobilization of low-level radioactive waste, *Appl. Environ. Microbiol.* 70 (2004) 6031.
- [9] M.L. Krumme, S.A. Boyd, Reductive dechlorination of chlorinated phenols in anaerobic upflow bioreactors, *Water Res.* 22 (1988) 171–177.
- [10] N. Takeda, K. Teranishi, Generation of superoxide anion radical from atmospheric organic matter, *Bull. Environ. Contam. Toxicol.* 40 (1988) 678–682.
- [11] S. Chaliha, K.G. Bhattacharyya, P. Paul, Catalytic destruction of 4-chlorophenol in water, *CLEAN–Soil Air Water* 36 (2008) 488–497.
- [12] M. Das, K.G. Bhattacharyya, Oxidative degradation of orange II dye in water with raw and acid-treated ZnO, and MnO₂, *CLEAN–Soil Air Water* 41 (2013) 984–991.
- [13] H. Yuan, X. Zhou, Y.-L. Zhang, Degradation of acid pharmaceuticals in the UV/H₂O₂ process: Effects of humic acid and inorganic salts, *CLEAN–Soil Air Water* 41 (2013) 43–50.
- [14] T. Qureshi, N. Memon, S.Q. Memon, M.A. Ashraf, Decontamination of ofloxacin: Optimization of removal process onto sawdust using response surface methodology, *Desalin. Water Treat.* (2015) 1–9, doi: 10.1080/19443994.2015.1006825.
- [15] Y. Abdollahi, A.H. Abdullah, U. Gaya, Z. Zainal, N. Yusof, Enhanced photodegradation of *o*-Cresol in aqueous Mn (1%)-doped ZnO suspensions, *Environ. Technol.* 33 (2011) 1183–1189.
- [16] Y. Abdollahi, A.H. Abdullah, Z. Zainal, N.A. Yusof, Photodegradation of *o*-Cresol by ZnO under UV irradiation, *J. Amer. Sci.* 7 (2011) 165–170.
- [17] Y. Abdollahi, A.H. Abdullah, A. Zakaria, Z. Zainal, H.R.F. Masoumi, N.A. Yusof, Photodegradation of *p*-Cresol in aqueous Mn (1%)-doped ZnO suspensions, *J. Adv. Oxid. Technol.* 15 (2012) 146–152.
- [18] Y. Abdollahi, A.H. Abdullah, U.I. Gaya, S. Ahmadzadeh, A. Zakaria, K. Shameli, Z. Zainal, H. Jahangirian, N.A. Yusof, Photocatalytic degradation of 1,4-benzoquinone in aqueous ZnO dispersions, *J. Braz. Chem. Soc.* 23 (2012) 236–240.
- [19] Y. Abdollahi, A. Zakaria, S. Nor Asrina, Degradation of high level *m*-Cresol by zinc oxide as photocatalyst, *CLEAN–Soil Air Water* 42 (2014) 1292–1297.

- [20] Y. Abdollahi, A.H. Abdullah, Z. Zainal, N.A. Yusof, Photodegradation of *p*-Cresol by zinc oxide under visible light, *Int. J. Appl. Sci. Technol.* 1 (2011) 99–105.
- [21] Y. Abdollahi, A.H. Abdullah, Z. Zainal, N.A. Yusof, Synthesis and characterization of manganese doped ZnO nanoparticles, *Int. J. Appl. Sci. Technol.* 11 (2011) 62–69.
- [22] B. Neppolian, H. Choi, S. Sakthivel, B. Arabindoo, V. Murugesan, Solar light induced and TiO₂ assisted degradation of textile dye reactive blue 4, *Chemosphere* 46 (2002) 1173–1181.
- [23] A. Hatipoğlu, An experimental and theoretical investigation of the photocatalytic degradation of *meta*-Cresol in TiO₂ suspensions: A model for the product distribution, *J. Photochem. Photobiol.* 165 (2004) 119–129.
- [24] I.K. Konstantinou, T.A. Albanis, TiO₂-assisted photocatalytic degradation of azo dyes in aqueous solution: kinetic and mechanistic investigations: A review, *Appl. Catal., B* 49 (2004) 1–14.
- [25] Y. Abdollahi, A.H. Abdullah, Z. Zainal, N.A. Yusof, Photocatalytic degradation of *p*-Cresol by zinc oxide under UV irradiation, *Int. J. Mol. Sci.* 13 (2011) 302–315.
- [26] Y. Abdollahi, A. Zakaria, A.H. Abdullah, H.R.F. Masoumi, H. Jahangirian, K. Shameli, M. Rezayi, S. Banerjee, T. Abdollahi, Semi-empirical study of *ortho*-Cresol photo degradation in manganese-doped zinc oxide nanoparticles suspensions, *Chem. Cent. J.* 6 (2012) 1–8.
- [27] Y. Abdollahi, A. Zakaria, K.A. Matori, K. Shameli, H. Jahangirian, M. Rezayi, T. Abdollahi, Interactions between photodegradation components, *Chem. Cent. J.* 6 (2012) 1–5.
- [28] D.C. Montgomery, *Design and Analysis of Experiments*, John Wiley & Sons, New York, NY, 2008.
- [29] A.I. Khuri, J.A. Cornell, *Response Surfaces: Designs and Analyses*, CRC, New York, NY, 1996.
- [30] Y. Lin, C. Ferronato, N. Deng, F. Wu, J.-M. Chovelon, Photocatalytic degradation of methylparaben by TiO₂: Multivariable experimental design and mechanism, *Appl. Catal., B* 88 (2009) 32–41.
- [31] I.-H. Cho, K.-D. Zoh, Photocatalytic degradation of azo dye (Reactive Red 120) in TiO₂/UV system: Optimization and modeling using a response surface methodology (RSM) based on the central composite design, *Dyes Pigm.* 75 (2007) 533–543.
- [32] J.C. Sin, S.M. Lam, A.R. Mohamed, Optimizing photocatalytic degradation of phenol by TiO₂/GAC using response surface methodology, *Korean J. Chem. Eng.* 28 (2011) 1–9.
- [33] R.H. Myers, D.C. Montgomery, C.M. Anderson-Cook, *Response Surface Methodology: Process and Product Optimization Using Designed Experiments*, vol. 705, John Wiley & Sons, New York, NY, 2009.
- [34] A.I. Khuri, S. Mukhopadhyay, *Response surface methodology*, *Wiley Interdisciplinary Rev.: Computat. Statist.* 2 (2010) 128–149.
- [35] D. Baş, İ.H. Boyacı, Modeling and optimization I: Usability of response surface methodology, *J. Food Eng.* 78 (2007) 836–845.
- [36] M.J. Anderson, P.J. Whitcomb, *RSM Simplified: Optimizing Processes Using Response Surface Methods for Design of Experiments*, Productivity Press, Virginia, VA, 2005.
- [37] G.W. Oehlert, *A First Course in Design and Analysis of Experiments*, vol. 1, WH Freeman, New York, NY, 2000.
- [38] S. Deming, Quality by design—part 3, *Chem. Tech.* 19 (1989) 249–255.
- [39] P.J. Whitcomb, M.J. Anderson, *RSM Simplified: Optimizing Processes Using Response Surface Methods for Design of Experiments*, Productivity Press, New York, NY, 2004.
- [40] R. Sen, T. Swaminathan, Response surface modeling and optimization to elucidate and analyze the effects of inoculum age and size on surfactin production, *Biochem. Eng. J.* 21 (2004) 141–148.
- [41] G.E.P. Box, K. Wilson, On the experimental attainment of optimum conditions, *J. Royal Stat. Soc. Series B (Methodological)* 13 (1951) 1–45.